



Enhanced Stem Cell Differentiation and Immunopurification of Genome Engineered Human Retinal Ganglion Cells

VALENTIN M. SLUCH¹,^a XITIZ CHAMLING,^b MELISSA M. LIU,^b CYNTHIA A. BERLINICKE,^b JIE CHENG,^b KATHERINE L. MITCHELL,^b DEREK S. WELSBIE,^{b,c} DONALD J. ZACK^{a,b,d,e}

Key Words. Stem cells • Retinal ganglion cells • Clustered regularly interspaced short palindromic repeats • Cell differentiation • Biotechnology

^aDepartment of Molecular Biology and Genetics, ^bDepartment of Ophthalmology, Wilmer Eye Institute, ^dThe Solomon H. Snyder Department of Neuroscience, ^eInstitute of Genetic Medicine, Johns Hopkins University School of Medicine, Baltimore, Maryland, USA; ^cShiley Eye Institute, University of California, San Diego, La Jolla, California, USA

Correspondence: Donald J. Zack, M.D., Ph.D., 400 N. Broadway, Smith Building, Room 3029, Baltimore, Maryland 21231, USA. Telephone: 410-502-5230; Fax: 410 502-5382; e-mail: dzack@jhmi.edu.; or Derek S. Welsbie, M.D., Ph.D., 9452 Medical Center Drive, Lower Level 3E417, Altman Clinical Translational Research Institute Building, La Jolla, California 92037, USA. Telephone: 858-822-3563; e-mail: dwelsbie@ucsd.edu

Received March 13, 2017; accepted for publication August 17, 2017; first published October 10, 2017.

<http://dx.doi.org/10.1002/sctm.17-0059>

This is an open access article under the terms of the Creative Commons Attribution-NonCommercial-NoDerivs License, which permits use and distribution in any medium, provided the original work is properly cited, the use is non-commercial and no modifications or adaptations are made.

ABSTRACT

Human pluripotent stem cells have the potential to promote biological studies and accelerate drug discovery efforts by making possible direct experimentation on a variety of human cell types of interest. However, stem cell cultures are generally heterogeneous and efficient differentiation and purification protocols are often lacking. Here, we describe the generation of clustered regularly-interspaced short palindromic repeats (CRISPR)-Cas9 engineered reporter knock-in embryonic stem cell lines in which tdTomato and a unique cell-surface protein, THY1.2, are expressed under the control of the retinal ganglion cell (RGC)-enriched gene *BRN3B*. Using these reporter cell lines, we greatly improved adherent stem cell differentiation to the RGC lineage by optimizing a novel combination of small molecules and established an anti-THY1.2-based protocol that allows for large-scale RGC immunopurification. RNA-sequencing confirmed the similarity of the stem cell-derived RGCs to their endogenous human counterparts. Additionally, we developed an in vitro axonal injury model suitable for studying signaling pathways and mechanisms of human RGC cell death and for high-throughput screening for neuroprotective compounds. Using this system in combination with RNAi-based knockdown, we show that knockdown of dual leucine kinase (DLK) promotes survival of human RGCs, expanding to the human system prior reports that DLK inhibition is neuroprotective for murine RGCs. These improvements will facilitate the development and use of large-scale experimental paradigms that require numbers of pure RGCs that were not previously obtainable. *STEM CELLS TRANSLATIONAL MEDICINE* 2017;6:1972–1986

SIGNIFICANCE STATEMENT

Pluripotent stem cells provide access to a large variety of human cell types. However, stem cell culture is often heterogeneous and efficient differentiation and purification of stem cell-derived cells are limited to relatively few examples. Via genetic engineering, we have generated stem cell reporter lines that enable the detection and purification of retinal ganglion cells (RGCs), an essential cell type for vision. Through modulation of known signaling pathways, we report an improved RGC differentiation protocol for high yields of purified RGCs. We also describe an siRNA protocol for exploration of signaling pathways in human RGCs.

INTRODUCTION

The retina and the brain are connected by the optic nerve, a structure composed of glial cells and retinal ganglion cell (RGC) axons. Axonal injury and death of RGCs, which can occur due to trauma or diseases such as glaucoma, lead to irreversible vision loss. The current treatment strategy for glaucoma, the second leading cause of blindness worldwide [1, 2], is based on lowering intraocular pressure (IOP) through pharmacological or surgical means, but IOP control is not always feasible, and even with significant IOP lowering RGC

loss can still progress [3]. In addition, IOP-independent RGC injury and cell death occur in a number of other diseases [4], such as dominant optic atrophy and Leber's hereditary optic neuropathy, diseases with a relatively early onset and no approved treatment options. A neuroprotective therapeutic strategy that promotes RGC function and survival could provide a novel approach appropriate for treatment of the whole group of RGC-related neurodegenerative diseases [5].

In addition to the use of model organisms for studies of disease, pluripotent stem cells (PSCs) can also be used to generate cell types of interest

in disease modeling efforts [6–10] and can, at times, reveal insights that are specific to the human system [10]. PSCs can be differentiated to retinal cells including RGCs using a growing number of protocols [11–18]. Using three-dimensional (3D) aggregate suspension cultures, it has become possible to form retinal organoids [11–13, 15, 19] that contain all of the expected retinal layers. When looking for structural developmental phenotypes, these 3D organoids provide a useful window into a world of human development that is otherwise difficult to access. However, in order to generate cells for large-scale cell type specific experiments, such as those used for drug screening, target discovery, and biochemical analysis, it is often advantageous to differentiate cells using high-throughput adherent protocols that maximize yield of the cells of interest.

As reported previously, we developed an adherent cell culture protocol for RGC differentiation using a CRISPR-Cas9 generated RGC reporter line in which the endogenous *BRN3B* (*POU4F2*) coding sequence was combined with the mCherry fluorescent protein gene via a P2A peptide [16]. While this reporter line is useful for RGC differentiation and isolation by fluorescence-activated cell sorting (FACS), the initial differentiation protocol that we reported is only of moderate efficiency and large-scale purification of the resulting RGCs has been challenging with this method because scaling with FACS is linear and is limited by the speed of the sorter. Additionally, FACS sorting of cells can induce cellular stress and can limit cell viability. In an effort to develop a simpler, more efficient, and easily scalable approach for generating large numbers of highly purified human RGCs, we have improved the efficiency of both the differentiation and RGC purification protocols. Here, we report a novel cell purification scheme based on CRISPR genome editing to generate a BRN3B-P2A-tdTomato-P2A-THY1.2 reporter line capable of RGC-specific immunopurification. Additionally, using a combination of differentiation promoting small molecules, we have improved our differentiation culture parameters to generate adherent cultures containing up to 50% of RGCs as a fraction of the total population of cells, demonstrated the transcriptional similarity of the resulting stem cell-derived RGCs to endogenous human RGCs, and developed a cell culture-based injury model suitable for high-throughput screening of RGC survival promoting molecules.

MATERIALS AND METHODS

Plasmid Construction

We used our previously generated [16] gRNA (Addgene plasmid #62988, Cambridge, MA, <https://www.addgene.org>) [20] for targeting *BRN3B* and a modified version of the donor plasmid template with a replacement of mCherry with tdTomato-P2A-THY1.2, that is, BRN3B-P2A-tdTomato-P2A-THY1.2. PCR was used to open the donor plasmid at the homology arms and to amplify the cDNAs of THY1.2 and tdTomato. All three pieces were assembled into one donor vector using Gibson Assembly (NEB, Ipswich, MA, <https://www.neb.com>). The stop codons of BRN3B and tdTomato were removed by design during PCR to allow for translation to continue through the P2A sites. The gRNA target genomic sequence is destroyed by

integration of the reporter into the genome and this sequence is not present in the homology template plasmids.

Reporter Line Generation

Gene editing of H7 or H9 (WiCell, Madison, WI, <https://www.wicell.org>) human embryonic stem cells (hESCs) was performed as previously described [16] with the following modifications. Electroporation was performed using the Neon Transfection System 10 μ L Kit (ThermoFisher Scientific, USA, <http://www.thermofisher.com>) according to the manufacturer's instructions. Briefly, hESCs were dissociated with TrypLE Express (ThermoFisher Scientific) and centrifuged to form a pellet of $150\text{--}250 \times 10^3$ cells. The cell pellet was resuspended in ice-cold R-buffer containing the plasmid encoding the gRNA and Cas9 and the donor plasmid. Electroporation was performed using the following parameters: voltage 1,100 V; interval 30 ms; 2 pulses. After electroporation, the cell suspension was transferred to low growth factor Matrigel (BD Biosciences, San Jose, CA, <http://www.bdbiosciences.com>) coated plates with mTeSR1 medium (Stemcell Technologies, Cambridge, MA, <https://www.stemcell.com>) containing 5 μ M blebbistatin (Sigma-Aldrich, USA, <http://www.sigmaaldrich.com>). These cells were subsequently passaged as single cells at a low density of 500 cells per well of a 6-well plate. The resulting stem cell colonies were individually picked and screened for reporter integration by PCR using the following forward and reverse primers (5'-3'):

forward: GGAGAAGCTGGACCTGAAGAAAAACGTGGTG
reverse: CCTGGTGAAATCTAAAATCTGAAGGGCAACAC

For BRN3B-H9 validation the following primers were used:

forward: GGAGAAGCTGGACCTGAAGAAAAACGTG
reverse: CCTGGTGAAATCTAAAATCTGAAGGG

The genomic region containing the integration site was amplified to determine zygosity for the reporter gene. We isolated one heterozygous reporter positive clone from H7 hESCs, named E4-H7. An additional homozygous BRN3B-P2A-tdTomato-P2A-THY1.2 reporter clone was isolated from H9 hESCs and named BRN3B-H9. All stem cell lines tested negative for predicted off-target mutations [16] and demonstrated a normal karyotype (Cell Line Genetics, Madison, WI, <https://www.clgenetics.com> and Cytogenetics Laboratory, Johns Hopkins Medical School, Baltimore, MD, <http://pathology.jhu.edu/cytogenetics>).

Human ESC Maintenance

Stem cells were maintained by clonal propagation in mTeSR1 media on growth factor-reduced Matrigel coated plates [21] at 10% CO₂/5% O₂. hESC colonies were passaged by dissociation with Accutase (Sigma-Aldrich) or TrypLE Express. mTeSR1 media containing 5 μ M blebbistatin was used for maintenance of single cells.

Human ESC Differentiation to RGCs

hESCs were dissociated to single cells and plated on Matrigel or Synthemax II-SC Substrate (Corning, USA, <https://www.corning.com>) coated plates at a density of 52.6 K/cm² in mTeSR1 with 5 μ M blebbistatin, a time point designated as day minus 1 (d-1). Unless otherwise specified, a Matrigel cover layer was not added to the cultures after plating. One day after plating, mTeSR1 was completely exchanged for N2B27 media [1:1 mix of DMEM/F12 and Neurobasal with 1 \times GlutaMAX Supplement, 1 \times antibiotic-antimycotic, 1% N2 Supplement, and 2% B27 Supplement (all from ThermoFisher Scientific)] to start differentiation; this day

was designated as day 0 (d0). Small molecules were added to the cells on day 1 (d1), 24 hours after d0. Small molecule addition was done in fresh N2B27 media. Cells were fed with a full exchange of N2B27 media every other day unless a small molecule was to be removed or added on that day of differentiation, requiring daily feeding. The following small molecules were aliquoted as 1,000× stocks in dimethyl sulfoxide (DMSO) and used at the working concentration noted in parentheses: Forskolin (FSK; 25 μM—Cell Signaling Technology, Danvers, MA, <https://www.cellsignal.com>), Dorsomorphin (1 μM—R&D Systems, Minneapolis, MN, <https://www.rndsystems.com>), IDE2 (2.5 μM—R&D Systems), DAPT (10 μM—Cell Signaling Technology), LDN-193189 (0.5 μM—Stemgent, Lexington, MA, <https://www.stemgent.com>), SB431542 (10 μM—Sigma-Aldrich). Nicotinamide (NIC; Sigma-Aldrich) was resuspended in water at 100× and used at a 10 mM working concentration. Noggin (ThermoFisher Scientific) was resuspended in 10 mM acetic acid with 0.5% bovine serum albumin (BSA) for a 1,000× stock and used at 100 ng/ml. All small molecules were added as indicated. Specifically, for our DIDNF+D protocol, Dorsomorphin and IDE2 (DID) were added from day 1 to 6, NIC from day 1 to 10, (FSK from day 1 to 30, and DAPT from day 18 to 30. Differentiation was carried out at 37°C in 5%CO₂/20% O₂.

DIDNF+D = Dorsomorphin+IDE2+Nicotinamide+Forskolin+DAPT

Fluorescence Microscopy

Fluorescence images were taken using the Eclipse TE-2000S inverted microscope (Nikon, Tokyo, Japan, <http://www.nikon.com>) or the EVOS FL Auto Cell Imaging System (ThermoFisher Scientific). The EVOS FL Auto Cell Imaging System was used for scanning whole well live culture plates. During imaging experiments, cells were maintained in a live cell chamber at 37°C with 5% CO₂ and 85% humidity.

Immunocytochemistry

BRN3B-H9-derived RGCs were used for analysis. These cells were differentiated to day 40 and purified using magnetic activated cell sorting (MACS). Cells were fixed with 4% paraformaldehyde in 0.2 M Sorenson's phosphate buffer (pH 7.4) for 10 minutes at room temperature, washed three times with PBS, permeabilized and blocked in 0.1% Triton X-100 in PBS with 5% BSA and 5% horse/goat serum for 1 hour at room temperature, and then incubated with primary antibody overnight at 4°C with 0.1% Triton X-100, 2% BSA, and 2% horse/goat serum in PBS. Primary antibodies used were TUJ1 (mouse, 1:2,000, Covance, MMS-435P, Princeton, NJ, <https://www.covance.com>) and RBPM5 (rabbit, 1:50, Santa Cruz Biotechnology, sc-133950, Dallas, TX, <https://www.scbt.com>). Cells were incubated with species-specific corresponding secondary antibodies for 45 minutes at room temperature. Secondary antibodies used were Alexa Fluor-488 and 647 conjugated antibodies (1:1,000, ThermoFisher Scientific). DAPI (4',6-diamidino-2-phenylindole, dihydrochloride, ThermoFisher Scientific) was used to stain nuclei. Washes after primary and secondary antibody staining were performed with 0.04% Triton X-100 in PBS. Fluorescence images were acquired with an EVOS FL Auto 2 Cell Imaging System (ThermoFisher Scientific).

High-Content Image Analysis

To quantify the total fluorescence area induced by small molecule treatment during differentiation, whole well images were taken

with a Cellomics ArrayScan VTI HCS Reader (ThermoFisher Scientific), and quantified using the SpotDetector Bioapplication.

Flow Cytometry and Fluorescence-Activated Cell Sorting

To set the sorting gates, we used identically differentiated reporter-less H7 or H9 hESCs to define the tdTomato+ or mCherry+ cell populations. Side scatter height versus width linear alignment filters were used to minimize cell aggregates. To prepare cells for flow cytometry, differentiated cultures were dissociated into a single cell suspension. Cultures were washed with phosphate buffered saline (PBS, pH 7.4), incubated with TrypLE Express for 15 minutes at 37°C, and then further incubated with Accumax (Sigma-Aldrich) for an additional 45 minutes. Following centrifugation, the cell pellet was resuspended in Live Cell Imaging Solution (ThermoFisher Scientific). The single cell suspension was then passed through a cell strainer (BD Biosciences) prior to analysis and sorting with an SH-800 Cell Sorter (Sony Biotechnology, San Jose, CA, <https://www.sonybiotechnology.com>). Following sorting, the cells were maintained in N2B27 with 10 μM FSK and 10 ng/ml CNTF (PeproTech, Rocky Hill, NJ, <https://www.peprotech.com>) on Matrigel coated plates.

Immunopanning of Human RGCs

Immunopanning was performed as described in Welsbie et al. [5]. Briefly, differentiated cells of day 35 or older were dissociated in the same manner as for flow cytometry analysis and then immunopanned on plates pre-conjugated with an anti-THY1.2 antibody (Bio-Rad, MCA02R, Hercules, CA, <https://www.bio-rad-antibodies.com>) or an anti-human THY1 antibody (EMD Millipore, USA, <http://www.emdmillipore.com>, F15-42-1) and goat anti-mouse IgM (Jackson ImmunoResearch, West Grove, PA, <https://www.jacksonimmuno.com>) at room temperature. After washing, bound cells were removed from the plate by a cell lifter and cultured on Matrigel coated dishes in N2B27 media. Flow cytometry was used to analyze the percentage of RGCs before and after panning.

MACS Purification of Human RGCs

Cells were prepared for MACS in the same manner as for flow cytometry/immunopanning. All reagents were purchased from Miltenyi Biotec (Auburn, CA, <http://www.miltenyibiotec.com>) and manufacturer instructions were followed. For cell numbers less than 50 million, MS columns were used, while LS columns were used to purify larger numbers of cells. CD90.2 (THY1.2) MicroBeads were added to the cell suspension and incubated at room temperature for 15 minutes for cell binding. To increase RGC purity, cells were generally run through one LS column followed by an MS column without additional supplementation of MicroBeads. Purity was assessed by flow cytometry using the previously determined fluorescence threshold.

RNA-Sequencing Analysis

BRN3B-H9-derived RGCs were used for analysis. These cells were differentiated to day 40 on Matrigel and purified using MACS. First strand cDNA synthesis was performed with 195 ng of total RNA using anchored oligo-dT and SuperScript III First-Strand Synthesis SuperMix (ThermoFisher Scientific). Second strand cDNA synthesis was performed using RNase H, DNA Polymerase I, and Invitrogen Second Strand Buffer (ThermoFisher Scientific). Double stranded cDNA was purified using DNA Clean & Concentrator-5 (Zymo Research, Irvine, CA, <https://www.zymoresearch.com>). Tagmentation was performed using the Nextera DNA Library Preparation Kit

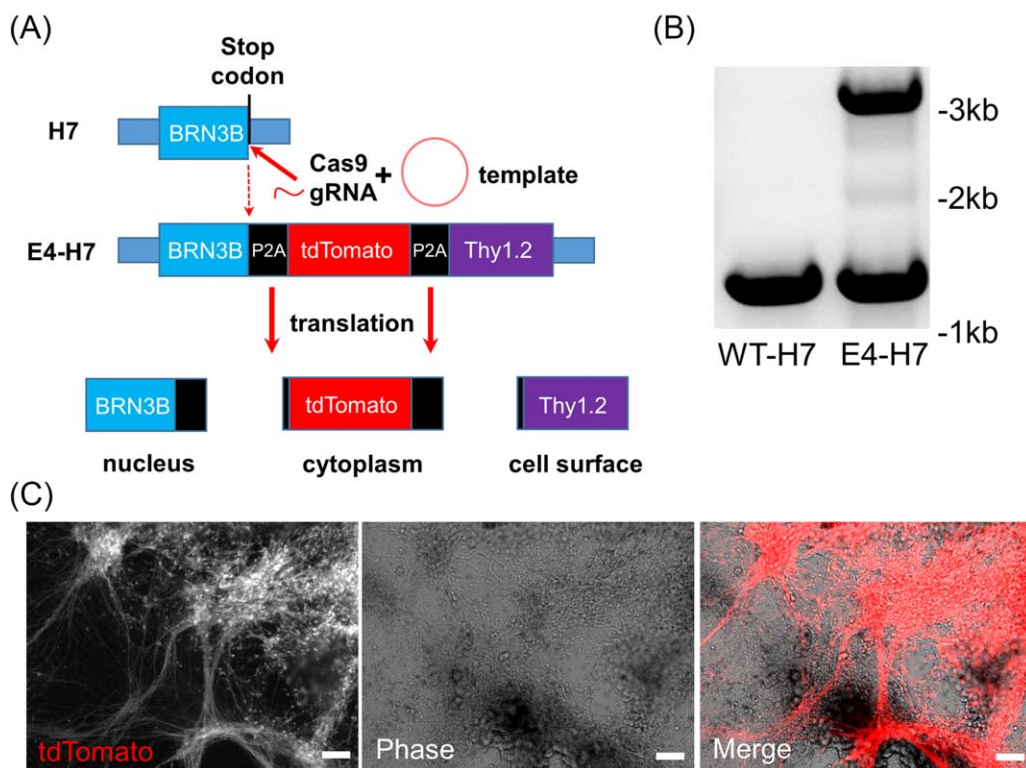


Figure 1. Generation of a novel retinal ganglion cell reporter stem cell line. **(A):** Schematic illustration depicting reporter design. CRISPR-Cas9 was used to target the stop codon of *BRN3B* in H7 hESCs. A P2A linked tdTomato was added in tandem with a P2A-THY1.2 to the *BRN3B* coding sequence. Following translation, the BRN3B transcription factor protein is localized to the nucleus, tdTomato to the cytoplasm, and THY1.2 to the cell surface. **(B):** PCR test for zygosity. Primers spanning the integration region were used to amplify genomic DNA for comparison between the parental WT H7 line and the isolated E4-H7 clone. E4-H7 DNA produced one band of expected integration size and one wild-type band, indicating heterozygosity of the modified locus. **(C):** Fluorescence microscopy of day 35 differentiated tdTomato⁺ cells. Scale bars = 100 μ m. Abbreviation: WT, wild type.

(Illumina, USA, <https://www.illumina.com>). Tagmented DNA was purified using DNA Clean & Concentrator-5 before Nextera PCR amplification. Libraries were cleaned using Agencourt AMPure XP beads according to the manufacturer instructions (Beckman Coulter, Indianapolis, IN, <https://www.beckman.com>). Libraries were evaluated by the High Sensitivity DNA Kit on the 2100 Bioanalyzer. They were then multiplexed and sequenced on an Illumina MiSeq with 76 bp paired end reads. Sequencing was performed to an average depth of approximately 8 million paired end reads per sample (range 7,085,422 to 8,829,967) and the average mapping rate was 70.2% (range 68.7 to 73.2). Reads were aligned to Gencode Release 24 (GRCh38.p5) using HISAT2 (v2.0.1-beta) [22]. Cuffquant and Cuffnorm (Cufflinks v2.2.1) were used to quantify expression levels and calculate normalized FPKM values [23]. We used the clustering function hclust and R version 3.2.2.

RGC Survival Assay

RGCs were immunopurified as described above and cultured in N2/B27 media in 96- or 384-well plates for 5 days. Cells were then challenged with colchicine, at the indicated concentration. At the time of injury, cells were either treated with tozasertib (BioVision, Milpitas, CA, <http://www.biovision.com>) or the vehicle control, or transfected with *DLK* versus control siPOOL (siTOOLS Biotech, Plannegg, Germany, <https://www.sitoolsbiotech.com>), using RNAiMAX (ThermoFisher Scientific) (50 nl per 96-well plate well, 30 nl per 384-well plate well). Survival was measured 48 hours later using

CellTiter-Glo (Promega, Madison, WI, <https://www.promega.com>), an ATP-based luminescence cell survival assay.

RESULTS

Generation of a Novel BRN3B Reporter Line Suitable for Immunopurification of RGCs

We sought to expand upon the utility of our previously described BRN3B-P2A-mCherry (A81-H7) reporter cell line [16] by developing a protocol for RGC isolation from stem cell culture that was not based on FACS in order to decrease the significant time required for purification, as well as to reduce the cell injury that can be induced by FACS. Since primary rodent RGCs are routinely immunopurified from culture using antibodies to the well-characterized RGC surface protein, THY1 [24], we explored whether the endogenously expressed human THY1 could be used for immunopanning of A81-H7-derived human RGCs. We first tested A81-H7-derived retinal cultures for binding to immunopanning plates coated with either anti-mouse THY1.2 or anti-human THY1 antibodies and found that only anti-human THY1 antibody coated plates were able to bind human stem cell-derived cells, demonstrating the species specificity of these antibodies (Supporting Information Fig. S1a). However, although BRN3B/mCherry positive cells did bind to anti-human THY1 antibody coated plates, more nonfluorescent cells resembling fibroblasts, a cell type known to express THY1 [25], were also bound, resulting in a lack of substantial RGC enrichment (Supporting Information Fig. S1b).

To generate an improved stem cell line in which differentiated RGCs could be more specifically isolated by immunopurification, we engineered a stem cell BRN3B-RGC reporter line with a surface antigen suitable for simple and efficient human RGC purification. We chose murine THY1.2 as an ideal antigen for this purpose for three reasons: (a) good anti-THY1.2 antibodies that do not bind to human cells are readily available (Supporting Information Fig. S1a), (b) methodology for THY1.2-based immunopurification is well established, and (c) THY1.2 is a relatively “non-foreign” protein for human RGCs because they already express a high similarity ortholog of this protein endogenously (THY1). In order to observe and immunopurify fluorescent RGCs while retaining normal BRN3B expression, we used P2A peptide sequences to link tdTomato [26] and THY1.2 with BRN3B in a single transcript (Fig. 1A). We utilized CRISPR-Cas9 genome editing and homology directed repair to modify H7 hESCs using a donor vector for the BRN3B-P2A-tdTomato-P2A-THY1.2 sequence and a gRNA targeting the *BRN3B* stop codon. Following transfection, one of seventy-two analyzed clones tested positive for correct reporter integration, a heterozygous clone that we named E4-H7 (Fig. 1B).

Reporter Line Differentiation and Immunopurification

We used our previously described protocol [16] to induce RGC differentiation of the E4-H7 cell line. As with our BRN3B-P2A-mCherry cultures, we first observed BRN3B+/tdTomato+ RGCs around day 25 of differentiation and additional fluorescent RGCs continued to emerge over time (Fig. 1C). We immunopanned the differentiated cells using anti-THY1.2 panning plates to purify a population of fluorescent RGCs that were >99% pure as assessed by flow cytometry and fluorescence microscopy (Fig. 2A, 2B).

Despite their high purity, the yield of isolated RGCs was sub-optimal (<50%) as a large number of fluorescent cells did not bind to the immunopanning plates (Fig. 2A, 2B). To increase yield, we tested an alternative immunopurification-based approach, MACS [27, 28]. In contrast to immunopanning, MACS purification resulted in increased RGC retention and yield (>70%), primarily by more efficiently binding the cells that expressed a lower level of tdTomato while maintaining a similarly high level of purity (>95%; Fig. 2C, 2D).

Development of an Improved and Simplified RGC Protocol

Building upon the above described improved purification strategy, we next wanted to further optimize and simplify the RGC differentiation protocol. Although our initial protocol involved two Matrigel coating steps (one to coat the plates followed by a second layer to cover the cells), we found that the second step was unnecessary. Simply pre-coating the plates with Matrigel yielded a similar <5% proportion of differentiated fluorescent RGCs (Supporting Information Fig. S2a) as we reported previously with the two-step procedure [16]. As with the A81-H7 line, RGC differentiation of E4-H7 cells was also significantly enhanced by the addition of FSK (Supporting Information Fig. S2a). Additionally, we augmented our protocol from plating hESC colony clusters in favor of plating defined numbers of dissociated single cells in order to decrease variability, establishing ~50,000 cells per cm² as the optimal density for RGC differentiation (Supporting Information Fig. S2b).

Since the *dual SMAD inhibition* protocol described by Chambers et al. [29] is known to efficiently generate neural progenitors of an anterior fate [29], we tested whether the combination of SB431542 and LDN-193189 [30], transforming growth factor beta

(TGF- β) and bone morphogenetic protein (BMP) pathways inhibitors, respectively, would increase the number of differentiating RGCs in our culture conditions. Counterintuitively, SB431542 inhibited retinal differentiation of fluorescent RGCs, an effect that was more pronounced with addition of LDN-193189 (Supporting Information Fig. S2c). Notably, Eiraku et al. [13] had previously reported SB431542-mediated suppression of Matrigel-induced spontaneous retinal differentiation, an effect that occurred potentially due to inhibition of Nodal, a member of the TGF- β family that acts through Activin receptors [31]. Therefore, we tested the effect of removing SB431542 while retaining BMP inhibition. Interestingly, the sole addition of the BMP inhibitor Dorsomorphin (DSM) [15] also decreased the number of RGCs produced in differentiation (Fig. 3A). This decrease could be due to the residual inhibition of Activin by DSM [32], a weaker inhibition than the one bestowed by SB431542, but an effect that could impact Nodal signaling. Additionally, the endogenous BMP signaling inhibitor protein, Noggin, also failed to increase RGC differentiation when added alone and actually appeared inhibitory to RGC genesis under our conditions (Fig. 3B).

Simultaneous Inhibition of BMP and Activation of Nodal Improves RGC Differentiation

We speculated that an increase in Nodal signaling could possibly diminish the inhibitory DSM effect on RGC differentiation. To test this hypothesis, we added IDE2, a small molecule capable of replacing Nodal in stem cell differentiation [33]. Although IDE2 was not able to increase RGC differentiation on its own (Fig. 3C, 3D), in combination with DSM or LDN-193189 it increased the number of RGCs in culture (Fig. 3D). Notably, when we applied the two small molecules together to cultures differentiated with a Matrigel cover layer, per our prior protocol [16], they did not have a positive effect on differentiation (Supporting Information Fig. S3a).

As the combination of DSM and IDE2 (DID) was most effective at promoting RGC differentiation, we further optimized the timing of addition of these small molecules. A time course of DID treatment established that these small molecules were best added during days 1 through 6 of our differentiation protocol (Supporting Information Fig. S3b, S3c).

DID Combination with NIC and FSK Further Drives RGC Differentiation and Can Replace Matrigel

While we were optimizing our DID conditions, we also tested whether the addition of NIC, a molecule implicated in neuronal as well as retinal pigment epithelium (RPE) differentiation [34–36], could be helpful to RGC genesis. Although NIC alone did not appear beneficial, we noticed an increase in RGC differentiation when NIC was combined with FSK (Supporting Information Fig. S4a, S4b). We then tested whether there would be a positive effect from addition of NIC and FSK (NF) to the DID cocktail, a combination we termed DIDNF. Indeed, DIDNF generated the most statistically significant percent increase of reporter positive cells, up to 20% (Fig. 4A).

Encouraged by the results with DIDNF, we tested whether this combination of molecules would be able to replace the need for Matrigel in RGC differentiation. Matrigel is an animal product that contains thousands of proteins [37] and exhibits significant lot to lot variability [38], making it less than ideal for protocol standardization and consistency. We tested Synthemax as a plate coating as it is an animal-free, synthetic, and defined substrate [39–41]. We

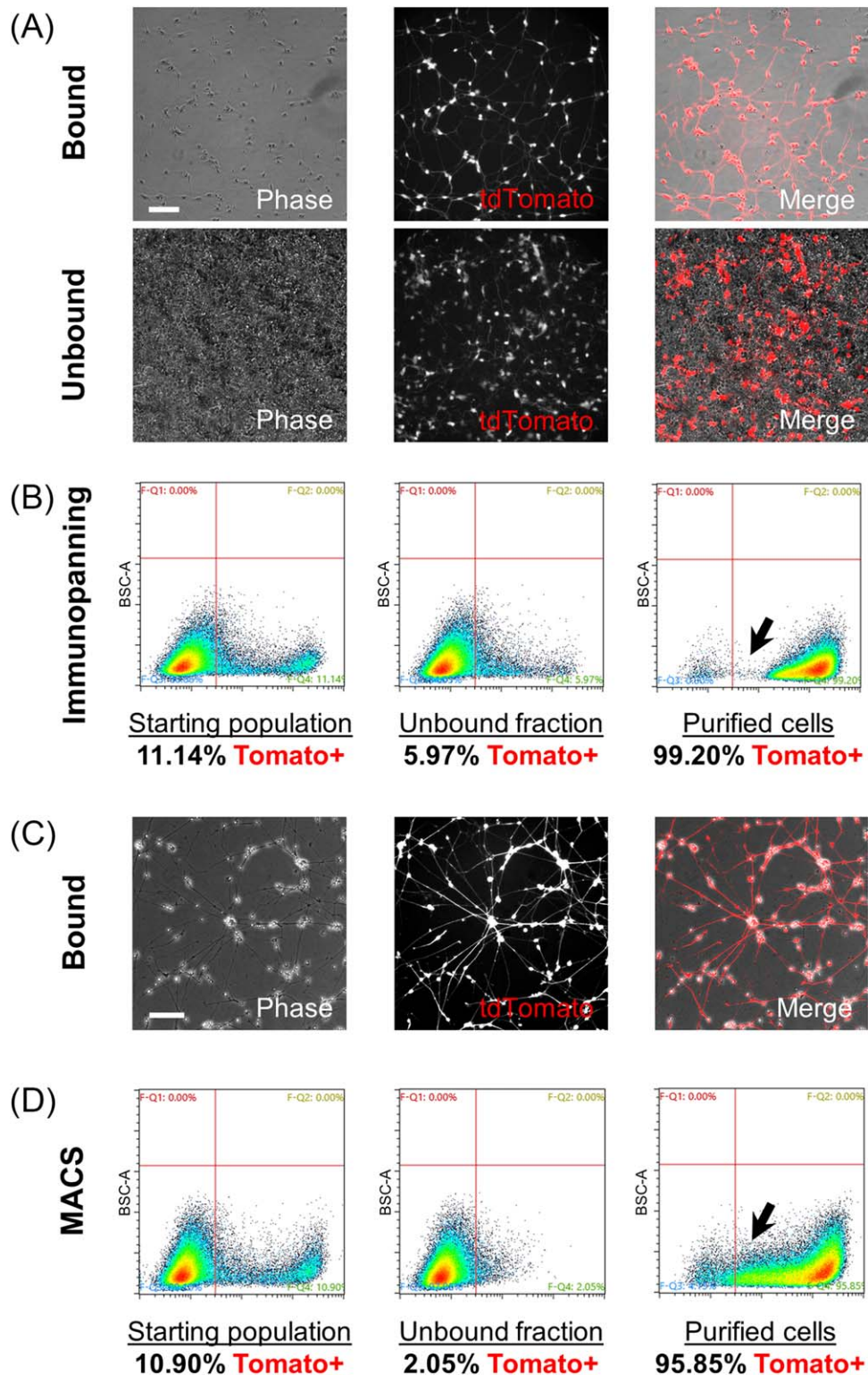


Figure 2. Immunopurification of differentiated stem cell-derived retinal ganglion cells. **(A):** Fluorescence and phase microscopy of cells after immunopanning purification. Fluorescent cells bound to anti-THY1.2 coated plates with high specificity. The unbound fraction contained non-fluorescent cells and cells of lower tdTomato fluorescence intensity. **(B):** Flow cytometry assessment of the immunopanning method. **(C):** Fluorescence and phase microscopy of cells after magnetic activated cell sorting (MACS) purification. **(D):** Flow cytometry assessment of the MACS method. Scale bars = 100 μ m. For flow cytometry, red fluorescence intensity is shown on the x-axis. Differentiated wild type H7 hESCs were used to set a gate threshold for tdTomato fluorescence. Higher fluorescence intensity cells are preferentially retained with the immunopanning method and lower fluorescence intensity cells are lost (black arrow). The MACS method retains more cells of a lower fluorescence intensity compared with immunopanning (black arrow). Abbreviation: BSC-A, back-scatter area.

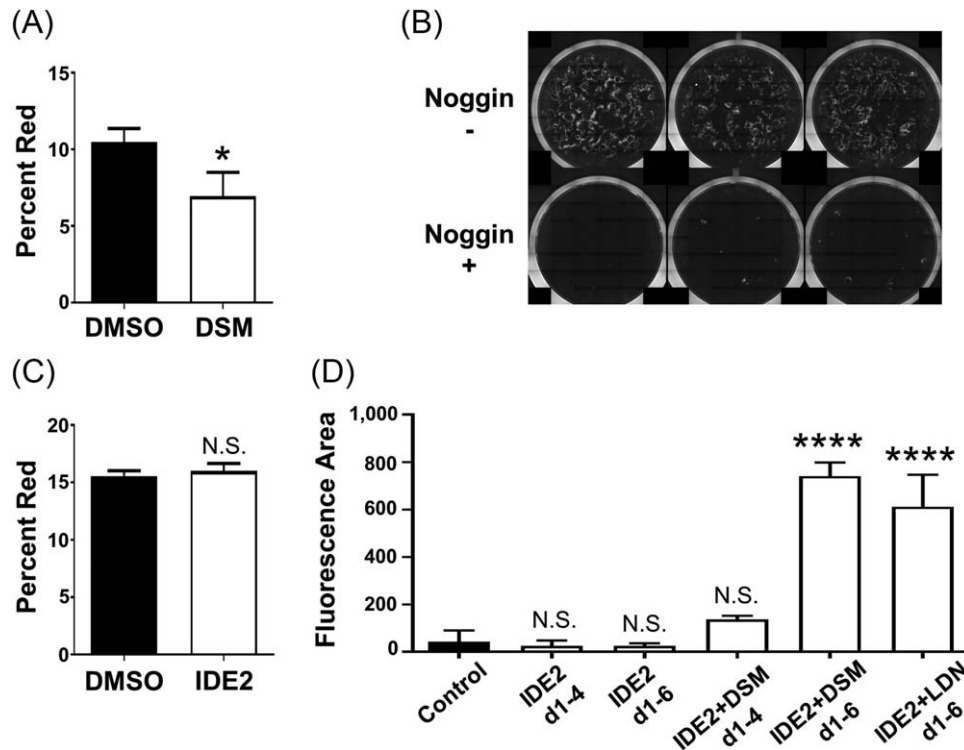


Figure 3. Effects of DSM, Noggin, and IDE2 on retinal ganglion cell differentiation. **(A):** Flow cytometry analysis of cells treated with DMSO or DSM from day 1 to 8 of differentiation. p value = .0258. **(B):** Whole-well fluorescence microscopy of differentiated cells with or without recombinant Noggin treatment for days 1 to 6. **(C):** Flow cytometry analysis of cells treated with DMSO or IDE2 from day 1 to 6 of differentiation. p value = .3888. **(D):** Cellomics scan of fluorescently differentiated cultures. IDE2, DSM, or LDN-193189 alone or in combinations were applied to cultures from day 1 to 4 or 1 to 6. Total fluorescence area was calculated. p values = .9951, .9960, .3145, .0001, and .0001, respectively. All cultures were analyzed on day 40–46. $N = 3$ where $N =$ independent experiments. *, $p < .05$; ****, $p < .0001$. N.S. = not significant. Unpaired two-tailed t test was used in (A) and (C) and One-way analysis of variance (ANOVA) ($\alpha = 0.05$ with Dunnett's multiple comparisons test) was used in (D). Error bars represent standard deviation. Abbreviation: DSM, Dorsomorphin.

observed little, if any, RGC differentiation on Synthemax coated plates in the absence of DIDNF (Fig. 4B, Supporting Information Fig. S4c, S4d). However, while the addition of DID or NF alone led to generation of a small number of RGCs on Synthemax, the full DIDNF combination led to an efficiency of RGC differentiation that was similar to that obtained with Matrigel, over 20% (Fig. 4B, Supporting Information Fig. S4c, S4d). Importantly, while NF did lead to a statistically significant increase in RGCs as a percentage of the population (Fig. 4B), NF resulted in low overall cell number, and DIDNF was needed to generate an RGC yield similar to that observed with Matrigel-assisted differentiation (Supporting Information Fig. S4c, S4d).

DAPT Further Improves Efficiency of RGC Differentiation

Since Notch signaling has been implicated in RGC development [42], and a number of stem cell studies have shown that Notch inhibition by N -[N -(3,5-Difluorophenacetyl)- L -alanyl]- s -phenylglycine t -butyl ester (DAPT) can increase RGC differentiation [43, 44], we tested whether addition of DAPT to the DIDNF protocol would further increase the efficiency of RGC generation. DAPT did not improve RGC yield when differentiation was carried out in the presence of a Matrigel cover layer (Supporting Information Fig. S5a). However, when differentiation was carried out without a Matrigel cover layer, DAPT did increase RGC generation efficiency when it was added from day 18 to 30, a window that we hypothesized would give retinal progenitors enough time to form and

then be biased toward the RGC lineage (Fig. 4C, Supporting Information Fig. S5b). Moreover, DAPT in combination with DID further increased RGC yield over DAPT or DID alone to values as high as 33%. Since the timing of DAPT addition was estimated, a time course for DAPT addition was then performed, which resulted in RGC percentages as high as 51.8% (Fig. 4D, Supporting Information Fig. S5c, S5d). We saw no benefit from starting DAPT treatment later than day 18 or from longer DAPT treatment past day 30; however, starting treatment earlier than day 16 appeared to be detrimental. Thus, the original DAPT addition from day 18 to 30 was incorporated as part of our optimized protocol (DIDNF+D; Fig. 4E).

Validation of DIDNF+D in Other Cell Lines

To determine whether our DIDNF+D differentiation protocol would work efficiently in other cell lines, we first validated the protocol in the BRN3B-P2A-mCherry (A81-H7) stem cell line (Fig. 5A). Then, we generated an additional reporter line from a different parental hESC population, H9 hESCs, using our BRN3B-P2A-tdTomato-THY1.2 donor plasmid (Supporting Information Fig. S6). Again, the small molecule cocktail increased RGC yield in this new BRN3B-H9 reporter line when differentiated on either Matrigel or Synthemax (Fig. 5A, 5B) with no apparent difference in cell morphology between the two plate coatings (Supporting Information Fig. S7). Additionally, as with E4-H7 cells, BRN3B-H9

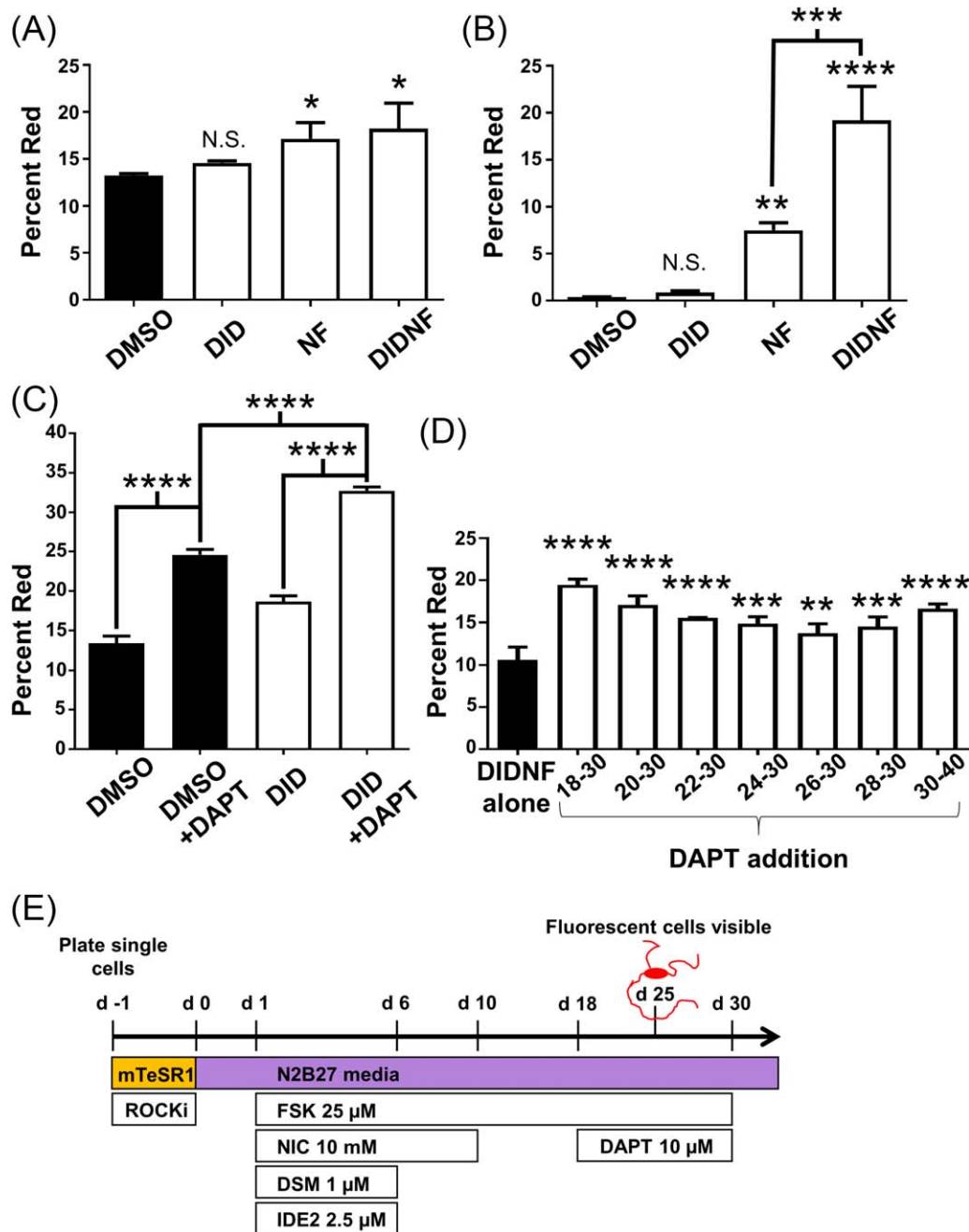


Figure 4. Differentiation improvement via addition of DID together with NF and DAPT. **(A):** Flow cytometry analysis of cells treated with DMSO, DID, NF, or DIDNF on Matrigel coated plates. DID and IDE2 were added from day 1 to 6, FSK from day 1 to 30. *p* values = .6219, .0431, and .0131, respectively. **(B):** Flow cytometry analysis of differentiated cells treated with DMSO, DID, NF, or DIDNF on Synthemax coated plates. Whole well fluorescence microscopy images of these cultures are shown in Supporting Information Figure S4d. *p* values = .9783, .0040, and .0001 for comparisons to DMSO and *p* value = .0003 for comparison of NF to DIDNF. **(C):** Flow cytometry analysis of differentiated cells treated with DMSO, DID, or their combination with DAPT added from day 18 to 30. All *p* values = <.0001. **(D):** Flow cytometry analysis of differentiated cells treated with DIDNF alone or in combination with DAPT added for the specified time period in days. *p* values = .0001, .0001, .0001, .0004, .0069, .0009, and .0001, respectively. **(E):** Schematic of the optimized protocol for RGC differentiation. All cultures were analyzed on day 40–45. *N* = 3 where *N* = independent experiments. *, *p* < .05; **, *p* < .01; ***, *p* < .001; ****, *p* < .0001. N.S. = not significant. ANOVA (α = 0.05) was used in (A–D); Dunnett's multiple comparisons test was used in (A), (B), and (D); Tukey's multiple comparisons test was used in (C) and to compare NF and DIDNF samples in (B). Error bars represent standard deviation. Abbreviations: DAPT, *N*-[*N*-(3,5-difluorophenacetyl)-*L*-alanyl]-*s*-phenylglycine *t*-butyl ester; DID, Dorsomorphin + IDE2; DIDNF, DID + NF; FSK, forskolin; NIC, nicotinamide; NF, nicotinamide + forskolin.

cells failed to differentiate to RGCs on Synthemax coated plates in the absence of the small molecule cocktail, and we were still able to successfully purify BRN3B-H9-derived RGCs

using anti-THY1.2 MACS methodology (Fig. 5C). While the differentiation percentage varied, these results demonstrate that the DIDNF+D protocol is active in several cell lines and is able

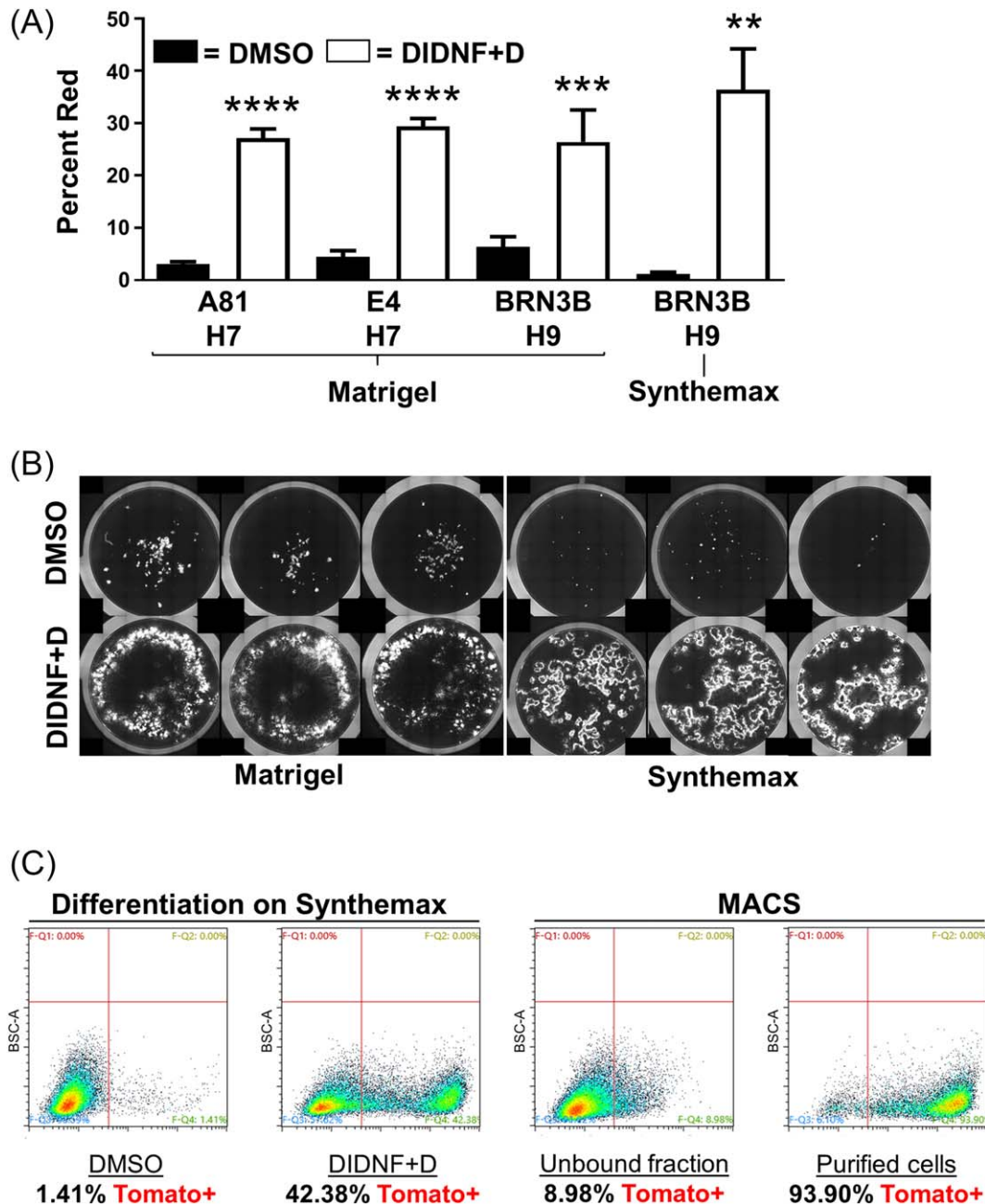


Figure 5. Validation of small molecule and purification strategy using additional reporter lines. **(A):** Flow cytometry analysis comparison of DIDNF+D differentiation using the A81-H7, E4-H7, and BRN3B-H9 cell lines on Matrigel and BRN3B-H9 on Synthemax. BRN3B-H9 analysis is of cultures shown in **(B)**. p values = <.0001, <.0001, .0008, and .0014, respectively. **(B)** Whole-well fluorescence microscopy images of differentiated cells from the BRN3B-H9 reporter cell line. Cells were treated with either DMSO or DIDNF+D on Matrigel or Synthemax coated plates. **(C):** Representative flow cytometry analysis of differentiation and subsequent MACS purification of Synthemax cultures in **(B)**. All cultures were analyzed on day 40. For A81-H7, E4-H7, and BRN3B-H9 on Synthemax $N = 3$. For BRN3B-H9 on Matrigel $N = 4$. $N =$ independent experiments. *, $p < .05$; **, $p < .01$; ***, $p < .001$; ****, $p < .0001$. Unpaired two-tailed t test was used to compare DMSO versus DIDNF+D for each line in **(A)**. Error bars represent standard deviation. Abbreviations: DIDNF+D = Dorsomorphin + IDE2 + Nicotinamide + Forskolin + DAPT; MACS, magnetic activated cell sorting.

to consistently generate cell populations that were approximately 20% to 50% RGCs.

RNA-Sequencing and Immunocytochemical Analysis of RGC Cell Fate and Differentiation

To assess the molecular similarity of the RGCs generated with our new small molecule supplemented protocol to RGCs

generated with our prior protocol [16], we compared the RGCs generated by the two protocols by RNA-sequencing-based gene expression profiling. We found that DIDNF+D differentiated tdTomato+ cells were highly similar to cells differentiated without small molecules, and confirmed that both populations expressed the expected RGC-associated genes (Fig. 6A, 6B). Additionally, we compared our RNA-sequencing data to published microarray data for the ganglion cell layer (GCL) and

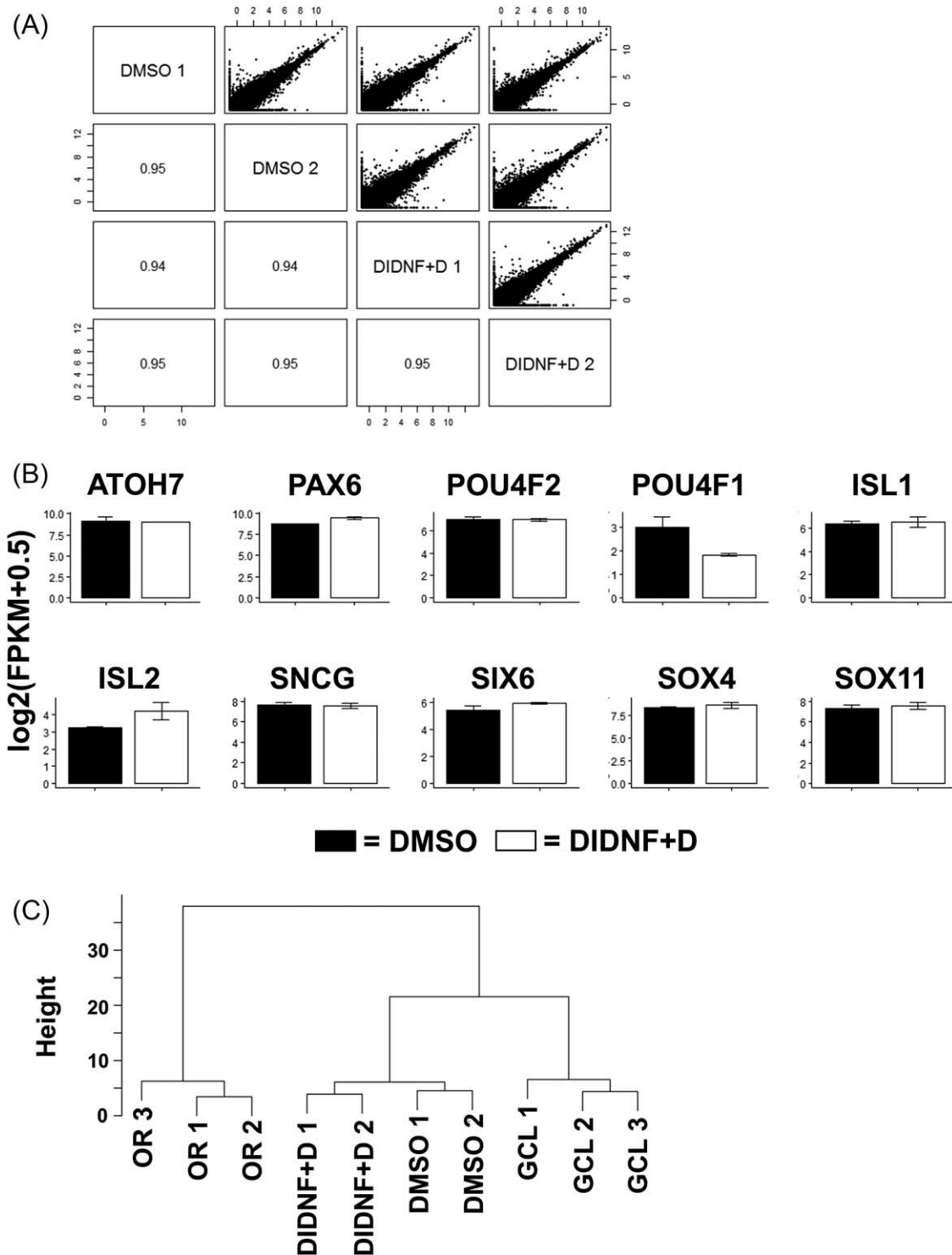


Figure 6. Gene expression analysis of retinal ganglion cell (RGCs) from small molecule driven differentiation. **(A):** Correlation of gene expression levels between DMSO and DIDNF+D treated samples measured by RNA-sequencing with two biological replicates per condition. Upper panel: pairwise plotting of $\log_2(\text{FPKM}+0.5)$. FPKM = fragments per kilobase per million mapped reads. Lower panel: Pearson correlation coefficient. **(B):** Gene expression in DMSO and DIDNF+D treated samples for selected RGC associated genes. **(C):** Hierarchical clustering of DMSO and DIDNF+D treated samples and GCL and OR collected by laser capture microdissection from human donors. Hierarchical clustering was performed using the Euclidean distance and complete linkage method. Abbreviations: DIDNF+D = Dorsomorphin + IDE2 + Nicotinamide + Forskolin + DAPT; GCL, ganglion cell layer; OR, outer retina.

outer retina (OR) fractions obtained from human donors by laser capture microdissection (LCM) [45]. Expression levels were averaged across microarray probes mapping to the same

gene. Only genes that were detected in both the RNA-sequencing and the microarray data sets were analyzed. The most differentially expressed genes between the GCL and OR

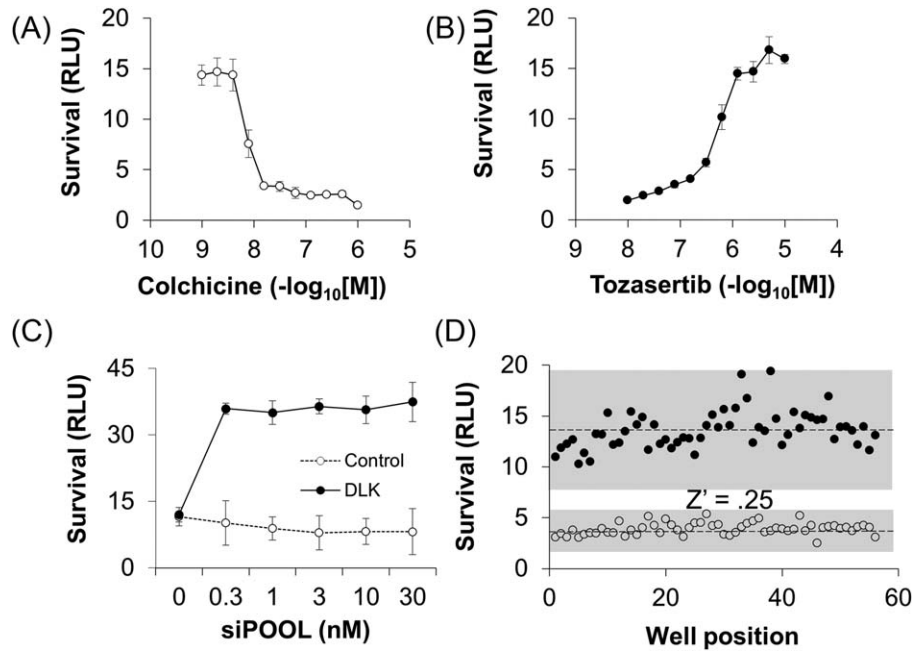


Figure 7. Stem cell-derived human retinal ganglion cell (RGCs) have conserved DLK-dependent injury signaling and are amenable to high-throughput screening. **(A, B):** Luminescence-based survival assay of immunopurified RGCs 48 hours after being challenged with increasing doses of colchicine (A) or a fixed dose of colchicine (1 μ M) and increasing doses of tozasertib (B). **(C, D):** Luminescence-based survival assay of immunopurified RGCs 48 hours after a colchicine challenge and transfection with increasing doses of control- or DLK-targeting siPOOLS (C) or 1 nM siPOOL (D). Assay validation— Z' determination. Solid black circles—DLK siPOOL, Open circles—control siPOOL. Shaded areas show three standard deviations from the mean (dashed line) of each population. $N = 3$ where $N =$ independent experiments. Error bars represent standard deviation. Abbreviations: DLK, dual leucine kinase; RLU, relative light units.

(q value < 0.1 and fold change > 10) were used for hierarchical clustering [46], which showed that despite the very different methods used, stem cell-derived RGCs showed high similarity to the LCM-isolated endogenous human RGC population (Fig. 6C).

After analyzing gene expression at the mRNA level by RNA-sequencing, we utilized immunocytochemistry to assess at the protein level the expression of the RGC marker RBPMS [47, 48] and the neuronal marker TUJ1 in the purified human RGCs generated using the DIDNF+D protocol. The stem cell-derived RGCs stained positive for both markers (Supporting Information Fig. S8), further supporting their RGC identity.

Development of a Stem Cell-Derived RGC Assay Suitable for Functional Genomic Screening

One potential use of human stem cell-derived RGCs is to screen for neuroprotective drugs and/or drug targets that promote RGC survival. Such neuroprotective strategies could be developed to complement current IOP-based treatments for glaucoma [49, 50], and additionally, they might be useful for the treatment of other optic neuropathies. We have previously used high-throughput functional genomic screening in primary mouse RGCs to identify dual leucine zipper kinase (DLK, MAP3K12) as a key mediator of axon injury signaling and RGC cell death [5, 51]. In this prior work, we also identified tozasertib, a protein kinase inhibitor with activity against DLK, as being neuroprotective for rodent RGCs in vitro and in vivo.

Building upon this earlier mouse RGC work, we sought to develop a human RGC-based injury assay that could be similarly used for disease modeling and drug development. As a stressor to

induce human RGC cell death we chose to challenge the cells with the microtubule destabilizer colchicine, which has previously been used to model axonal injury [52–55]. Two days after colchicine challenge, a dose-response curve for viability was generated using the CellTiter-Glo luminescence-based cell survival assay (Fig. 7A). Based upon these results, we chose a dose of 1 μ M colchicine for assay development as this dose resulted in a plateau of approximately 70%–90% human RGC cell death. We then tested whether human stem cell-derived RGCs recapitulated the injury signaling seen in rodents by pharmacologically and genetically inhibiting DLK. Consistent with our previous murine RGC results [5], tozasertib impressively promoted human RGC survival (Fig. 7B).

We also optimized siRNA-based knockdown of gene expression in the human RGCs to be able to explore cell-signaling pathways. For these studies, we utilized a system of high-complexity pooled siRNAs (siPOOLS) that are designed to limit off-target effects [56]. Again, consistent with our previous murine RGC results [5], DLK siPOOL increased survival of the human RGCs (Fig. 7C). Finally, we leveraged the activity of the DLK siPOOL in order to validate the feasibility of performing a high-throughput functional genomic screen with the human RGCs. Using automated liquid handling, stem cell-derived RGCs were seeded into a section of a 384-well plate, transfected with DLK versus control siPOOL and then assayed for survival 2 days after colchicine challenge (Fig. 7D). By measuring the variation in survival for the negative (i.e., control siPOOL transfected) and positive control (i.e., DLK siPOOL transfected) cell populations, we determined that the platform had a Z' of 0.25, a reasonable value given the cellular variability of stem cell-derived neurons, and far greater than our initial primary RGC-based screen [5]. Taken together, these results suggest that DLK-mediated axon injury signaling is conserved in

human stem cell-derived RGCs and that future functional genomic screens could reliably detect novel pathway members.

DISCUSSION

The use of stem cell-derived cells for research that requires large numbers of cells, such as high-throughput drug discovery or biochemical inquiry, is often hindered by a lack of robust differentiation and purification techniques suitable for generating sufficient numbers of the relevant cell types of interest. As one example, although human RGCs are a medically relevant cell type that presents many opportunities for drug discovery [57] and stem cell differentiation to RGCs has been reported by a number of groups [11–14, 16, 17, 58, 59], large-scale production of purified RGCs from stem cell culture remains challenging. The challenges include the limited efficiency of available differentiation protocols and problems associated with the scalability of the purification methods, which can require slow and expensive equipment in the case of FACS.

To address these limitations, we designed a novel RGC reporter cell line that allows for large-scale affinity isolation of highly purified human RGCs. We used CRISPR-Cas9 technology to knock in a P2A-tdTomato-P2A-THY1.2 sequence into the *BRN3B* locus, creating a unique surface antigen expressed with the cell type specificity of a transcription factor. We generated two such reporter lines, heterozygous E4-H7 and homozygous BRN3B-H9. Upon retinal differentiation of these cells, tdTomato+ fluorescent RGCs are generated that are capable of immunopurification via anti-THY1.2 antibody coated plates (immunopanning) or conjugated microbeads (MACS) in a much more efficient and accelerated manner than previously possible with FACS technology. Notably, during the preparation of this manuscript, Gill et al. described the use of MACS for endogenous THY1 to isolate human RGCs from a 3D stem cell differentiation culture [17]. However, as shown here and by Gill et al., standard THY1-based purification schemes of human stem cell cultures do not yield highly purified RGC populations because the cultures also contain significant numbers of non-RGC, THY1+ cells.

The combination of genome editing, enhanced RGC differentiation, and MACS technology described here makes possible the isolation of a billion, or more, highly purified human RGCs. Cell numbers of this magnitude are practically unattainable with primary murine RGC culture. For comparison, with our differentiation protocol a single 6-well plate of stem cell culture yields approximately 80 million cells. If we assume a low end RGC fraction of 20%, then using MACS one would be able to conservatively purify more than 10 million human RGCs from one 6-well plate. A culture of 10 million cells would require the sacrifice and laborious dissection of more than 80 mice to generate an equal number of primary RGCs, assuming 100% yield and an average of 60,000 RGCs per mouse retina [60]. Thus, even in this smaller range, our system of human stem cell-derived RGCs offers clear practical advantages over primary murine RGC cultures in terms of scale and ease of isolation. It should also be noted that the THY1.2 purification strategy is not limited to RGCs. As these antibodies are highly species specific and perform exceptionally well within the stem cell differentiation system, theoretically any cell type of interest could be targeted for affinity purification using CRISPR and MACS technologies.

In addition to developing a simple, fast, and efficient protocol for stem cell-derived RGC purification, we have also improved the efficiency of RGC differentiation, up to 50% efficiency, from our

previous protocol, which generally showed 10% or lower efficiency. This increased efficiency was achieved by optimizing the addition of DSM, IDE2, NIC, FSK, and DAPT, a combination we termed DIDNF+D. We added DSM (BMP inhibitor) and IDE2 (Nodal activator) to our differentiation culture based on the hypothesis that the *dual SMAD* differentiation protocol [29] was prohibitive to retinal genesis due to its inhibition of Nodal signaling. The need for Nodal signaling in retinal development has been highlighted previously. For example, it has been shown that inhibition of Nodal/Activin directs differentiation toward a caudal identity, that is, away from retinal development [61]. Moreover, zebrafish and mice with Nodal mutations display defects in eye development such as cyclopia [62, 63] as well as loss of *ath5* (*ATOH7*) expression [64], an essential gene for RGC development [65, 66]. Furthermore, recently a role for Nodal/Activin signaling in establishment of the eye field has been described in hESC [67] and mESC differentiation [68] and addition of IDE1, another Nodal agonist molecule similar to IDE2, has been used to enhance stem cell differentiation to RPE [69]. Surprisingly, we noticed that DSM alone decreased RGC differentiation, perhaps due to its weaker activity against Activin/Nodal [32]. Similarly, IDE2 alone did not increase RGC genesis, possibly due to the presence of Matrigel inducing enough Nodal signaling to promote peak differentiation. Strikingly, the combination of DSM with IDE2 (DID) did lead to increased RGC differentiation, suggesting that IDE2-increased Nodal signaling could compensate for DSM-induced inhibition of this pathway. Although more selective inhibitors of the BMP pathway could potentially improve differentiation over DSM [70], DSM performed slightly better than LDN-193189 when combined with IDE2 and the BMP inhibitor protein Noggin did not drive RGC differentiation either, likely due to its own reported inhibition of Nodal [71]. Therefore, a combinatorial approach to differentiation such as we applied here may be the best current strategy as it appears to be difficult to exclusively inhibit the BMP pathway.

The timing of addition of DSM and IDE2 also proved crucial for retinal differentiation. During optimization, we found that these molecules promoted RGC differentiation best when added from day 1 to day 6. Interestingly, it has recently been reported that BMP4 addition to optic cup differentiation cultures increases retinal genesis if added on day 6 [72], when further BMP inhibition would likely be detrimental [73]. In addition to utilizing the DID small molecule combination to promote differentiation to RGCs, we also observed that these molecules were additive with the previously identified FSK [16] and NIC [34–36, 69] (DIDNF). Notably, together these molecules could induce RGC differentiation in the absence of Matrigel, an outcome that was not possible without them in adherent culture. Moreover, since we used a chemically defined plate coating, Synthamax, the differentiation protocol became nearly xeno-free. The only remaining animal product in our protocol is the bovine serum albumin that is present in B27, and it can be replaced with human serum albumin if desired for a truly xeno-free system. Thus, our small molecule directed differentiation protocol allows for the production of RGCs in a completely chemically defined manner that could decrease variability and could potentially be used in future clinical cell-based applications [74, 75].

To improve our protocol further, we added the Notch signaling inhibitor DAPT to promote differentiation of retinal progenitors toward RGCs [43, 44]. Importantly, during the initial optimization of our protocol, we removed the Matrigel cover layer that we used for prior differentiation experiments [16], and only retained a Matrigel plate coating. In these conditions, DAPT resulted in an increase in RGC genesis and synergized with DIDNF, thus making

the protocol DIDNF+D. Notably, the DAPT-induced RGC increase was nullified by a Matrigel cover layer, an observation that may explain the findings of Nakano et al. where a Matrigel cover layer was also used and DAPT had no effect on RGC differentiation [12].

RNA-sequencing analysis revealed very little difference in gene expression between the purified RGC populations induced by the small molecules as compared with controls, suggesting that these small molecules drive the natural differentiation process. It will be interesting to determine if additional small molecules could alter the generated RGC population and reveal underlying regulators of RGC subtype specification. Similar to *BRN3B*, *BRN3A* and *BRN3C* have gRNA target sites around their stop codons with very few predicted off-targets, creating an ideal situation for reporter line creation using the method described herein. Using multiplexed *BRN3A* and *BRN3C* reporters in combination with *BRN3B* should allow for purification of RGC subtypes for further analysis [76, 77]. Likewise, an OPN4-P2A-tdTomato-P2A-THY1.2 reporter cell line for isolation of intrinsically photosensitive RGCs [78] expressing melanopsin (OPN4) could be generated.

CONCLUSION

To test one potential application of our highly-purified population of human RGCs, we developed a cell death survival assay by treating RGCs with colchicine to induce cell death, and then rescued the cells by pharmacologic and genetic inhibition of DLK [5]. We then used this approach to optimize a high-throughput siRNA-based screening platform and showed that we could detect known positive hits. Given that our methodology is capable of producing large numbers of human RGCs, this should enable kinome-scale or potentially genome-scale screens for novel neuroprotective drug targets. A similar high-throughput platform can also be combined with small molecule libraries to identify putative neuroprotective compounds. Moreover, through utilization of

CRISPR-generated reporters in conjunction with high-content imaging, other phenotypic parameters could be assessed in a similar manner, for example, screening for mediators of neurite outgrowth or degeneration.

ACKNOWLEDGMENTS

We thank Hans Bjornsson for allowing us to use his MiSeq instrument, Li Zhang for providing training and help with the RNA-sequencing experiment, and Gabrielle Cannon and Loyal Goff for assistance with the RNA-sequencing run. This research was supported by grants from the Maryland Stem Cell Research Fund (2014-MSCRFI-0774), NIH (T32-90040730, 1R01EY02268001, 5T32EY007143, 5P30EY001765, and R01EY023754), BrightFocus Foundation, and unrestricted funds from Research to Prevent Blindness, Inc., and generous gifts from the Guerrieri Family Foundation and from Mr. and Mrs. Robert and Clarice Smith.

AUTHOR CONTRIBUTIONS

V.M.S. and D.S.W.: conception and design, collection and assembly of data, data analysis and interpretation, manuscript writing, final approval of manuscript; X.C. and M.M.L.: collection and assembly of data, data analysis and interpretation, manuscript writing, final approval of manuscript; C.A.B.: collection and assembly of data, data analysis and interpretation; J.C. and K.L.M.: collection and assembly of data; D.J.Z.: conception and design, collection and assembly of data, data analysis and interpretation, manuscript writing, financial support, administrative support, final approval of manuscript.

DISCLOSURE OF POTENTIAL CONFLICTS OF INTEREST

The authors indicated no potential conflicts of interest.

REFERENCES

- Kingman S. Glaucoma is second leading cause of blindness globally. *Bull World Health Org* 2004;82:887–888.
- Sluch VM, Zack DJ. Stem cells, retinal ganglion cells and glaucoma. *Dev Ophthalmol* 2014;53:111–121.
- Fernandes KA, Harder JM, Williams PA et al. Using genetic mouse models to gain insight into glaucoma: Past results and future possibilities. *Exp Eye Res* 2015;141:42–56.
- Levin LA, Gordon LK. Retinal ganglion cell disorders: Types and treatments. *Prog Retin Eye Res* 2002;21:465–484.
- Welsbie DS, Yang Z, Ge Y et al. Functional genomic screening identifies dual leucine zipper kinase as a key mediator of retinal ganglion cell death. *Proc Natl Acad Sci USA* 2013; 110:4045–4050.
- Nageshappa S, Carrone C, Trujillo CA et al. Altered neuronal network and rescue in a human MECP2 duplication model. *Mol Psychiatry* 2015;21:178–188.
- Sandoe J, Eggan K. Opportunities and challenges of pluripotent stem cell neurodegenerative disease models. *Nat Neurosci* 2013; 16:780–789.
- Kiskinis E, Sandoe J, Williams LA et al. Pathways disrupted in human ALS motor neurons identified through genetic correction of mutant SOD1. *Cell Stem Cell* 2014;14:781–795.
- Mariani J, Coppola G, Zhang P et al. FOXG1-Dependent dysregulation of GABA/glutamate neuron differentiation in autism spectrum disorders. *Cell* 2015;162:375–390.
- Mertens J, Stuber K, Wunderlich P et al. APP processing in human pluripotent stem cell-derived neurons is resistant to NSAID-based gamma-secretase modulation. *Stem Cell Reports* 2013;1:491–498.
- Zhong X, Gutierrez C, Xue T et al. Generation of three-dimensional retinal tissue with functional photoreceptors from human iPSCs. *Nat Commun* 2014;5:4047.
- Nakano T, Ando S, Takata N et al. Self-formation of optic cups and storable stratified neural retina from human ESCs. *Cell Stem Cell* 2012;10:771–785.
- Eiraku M, Takata N, Ishibashi H et al. Self-organizing optic-cup morphogenesis in three-dimensional culture. *Nature* 2011;472: 51–56.
- Tanaka T, Yokoi T, Tamalu F et al. Generation of retinal ganglion cells with functional axons from human induced pluripotent stem cells. *Sci Rep* 2015;5:8344.
- Meyer JS, Howden SE, Wallace KA et al. Optic vesicle-like structures derived from human pluripotent stem cells facilitate a customized approach to retinal disease treatment. *STEM CELLS* 2011;29:1206–1218.
- Sluch VM, Davis CH, Ranganathan V et al. Differentiation of human ESCs to retinal ganglion cells using a CRISPR engineered reporter cell line. *Sci Rep* 2015;5:16595.
- Gill KP, Hung SS, Sharov A et al. Enriched retinal ganglion cells derived from human embryonic stem cells. *Sci Rep* 2016;6: 30552.
- Crombie DE, Daniszewski M, Liang HH et al. Development of a modular automated system for maintenance and differentiation of adherent human pluripotent stem cells. *SLAS Discov* 2017;22:1016–1025.
- Volkner M, Zschatzsch M, Rostovskaya M et al. Retinal organoids from pluripotent stem cells efficiently recapitulate retinogenesis. *Stem Cell Reports* 2016;6:525–538.
- Ran FA, Hsu PD, Wright J et al. Genome engineering using the CRISPR-Cas9 system. *Nat Protoc* 2013;8:2281–2308.
- Maruotti J, Wahlin K, Gorrell D et al. A simple and scalable process for the differentiation of retinal pigment epithelium from human pluripotent stem cells. *STEM CELLS TRANSLATIONAL MEDICINE* 2013;2:341–354.
- Kim D, Langmead B, Salzberg SL. HISAT: A fast spliced aligner with low memory requirements. *Nat Methods* 2015;12:357–360.

- 23 Trapnell C, Williams BA, Pertea G et al. Transcript assembly and quantification by RNA-Seq reveals unannotated transcripts and isoform switching during cell differentiation. *Nat Biotechnol* 2010;28:511–515.
- 24 Barres BA, Silverstein BE, Corey DP et al. Immunological, morphological, and electrophysiological variation among retinal ganglion cells purified by panning. *Neuron* 1988;1:791–803.
- 25 Koumas L, Smith TJ, Feldon S et al. Thy-1 expression in human fibroblast subsets defines myofibroblastic or lipofibroblastic phenotypes. *Am J Pathol* 2003;163:1291–1300.
- 26 Day RN, Davidson MW. The fluorescent protein palette: Tools for cellular imaging. *Chem Soc Rev* 2009;38:2887–2921.
- 27 Miltenyi S, Muller W, Weichel W et al. High gradient magnetic cell separation with MACS. *Cytometry* 1990;11:231–238.
- 28 Grutzkau A, Radbruch A. Small but mighty: How the MACS-technology based on nanosized superparamagnetic particles has helped to analyze the immune system within the last 20 years. *Cytometry A* 2010;77:643–647.
- 29 Chambers SM, Fasano CA, Papapetrou EP et al. Highly efficient neural conversion of human ES and iPS cells by dual inhibition of SMAD signaling. *Nat Biotechnol* 2009;27:275–280.
- 30 Maroof AM, Keros S, Tyson JA et al. Directed differentiation and functional maturation of cortical interneurons from human embryonic stem cells. *Cell Stem Cell* 2013;12:559–572.
- 31 Shen MM. Nodal signaling: Developmental roles and regulation. *Development* 2007;134:1023–1034.
- 32 Zhou J, Su P, Li D, Tsang S et al. High-efficiency induction of neural conversion in human ESCs and human induced pluripotent stem cells with a single chemical inhibitor of transforming growth factor beta superfamily receptors. *STEM CELLS* 2010;28:1741–1750.
- 33 Borowiak M, Maehr R, Chen S et al. Small molecules efficiently direct endodermal differentiation of mouse and human embryonic stem cells. *Cell Stem Cell* 2009;4:348–358.
- 34 Maruotti J, Sripathi SR, Bharti K et al. Small-molecule-directed, efficient generation of retinal pigment epithelium from human pluripotent stem cells. *Proc Natl Acad Sci USA* 2015;112:10950–10955.
- 35 Griffin SM, Pickard MR, Orme RP et al. Nicotinamide promotes neuronal differentiation of mouse embryonic stem cells in vitro. *Neuroreport* 2013;24:1041–1046.
- 36 Idelson M, Alper R, Obolensky A et al. Directed differentiation of human embryonic stem cells into functional retinal pigment epithelium cells. *Cell Stem Cell* 2009;5:396–408.
- 37 Hughes CS, Postovit LM, Lajoie GA. Matrigel: A complex protein mixture required for optimal growth of cell culture. *Proteomics* 2010;10:1886–1890.
- 38 Villa-Diaz LG, Ross AM, Lahann J et al. Concise review: The evolution of human pluripotent stem cell culture: From feeder cells to synthetic coatings. *STEM CELLS* 2013;31:1–7.
- 39 Pennington BO, Clegg DO, Melkounian ZK et al. Defined culture of human embryonic stem cells and xeno-free derivation of retinal pigmented epithelial cells on a novel, synthetic substrate. *STEM CELLS TRANSLATIONAL MEDICINE* 2015;4:165–177.
- 40 Baranov P, Regatieri C, Melo G et al. Synthetic peptide-acrylate surface for self-renewal of human retinal progenitor cells. *Tissue Eng Part C Methods* 2013;19:265–270.
- 41 Jin S, Yao H, Weber JL et al. A synthetic, xeno-free peptide surface for expansion and directed differentiation of human induced pluripotent stem cells. *PLoS One* 2012;7:e50880.
- 42 Nelson BR, Gumuscu B, Hartman BH et al. Notch activity is downregulated just prior to retinal ganglion cell differentiation. *Dev Neurosci* 2006;28:128–141.
- 43 Xie BB, Zhang XM, Hashimoto T et al. Differentiation of retinal ganglion cells and photoreceptor precursors from mouse induced pluripotent stem cells carrying an Atoh7/Math5 lineage reporter. *PLoS One* 2014;9:e112175.
- 44 Riazifar H, Jia Y, Chen J et al. Chemically induced specification of retinal ganglion cells from human embryonic and induced pluripotent stem cells. *STEM CELLS TRANSLATIONAL MEDICINE* 2014;3:424–432.
- 45 Kim CY, Kuehn MH, Clark AF et al. Gene expression profile of the adult human retinal ganglion cell layer. *Mol Vis* 2006;12:1640–1648.
- 46 Storey JD, Tibshirani R. Statistical significance for genomewide studies. *Proc Natl Acad Sci USA* 2003;100:9440–9445.
- 47 Rodriguez AR, de Sevilla Müller LP, Brecha NC. The RNA binding protein RBPMS is a selective marker of ganglion cells in the mammalian retina. *J Comp Neurol* 2014;522:1411–1443.
- 48 Kwong JM, Caprioli J, Piri N. RNA binding protein with multiple splicing: A new marker for retinal ganglion cells. *Invest Ophthalmol Vis Sci* 2010;51:1052–1058.
- 49 Levin LA, Peeples P. History of neuroprotection and rationale as a therapy for glaucoma. *Am J Manag Care* 2008;14(suppl 1):S11–14.
- 50 Tian K, Shibata-Germanos S, Pahlitzsch M et al. Cordeiro MF. Current perspective of neuroprotection and glaucoma. *Clin Ophthalmol* 2015;9:2109–2118.
- 51 Welsbie DS, Mitchell KL, Jaskula-Ranga V et al. Enhanced functional genomic screening identifies novel mediators of dual leucine zipper kinase-dependent injury signaling in neurons. *Neuron* 2017;94:1142–1154.e1146.
- 52 Bounoutas A, Kratz J, Emtage L et al. Microtubule depolymerization in *Caenorhabditis elegans* touch receptor neurons reduces gene expression through a p38 MAPK pathway. *Proc Natl Acad Sci USA* 2011;108:3982–3987.
- 53 Miller BR, Press C, Daniels RW et al. A dual leucine kinase-dependent axon self-destruction program promotes Wallerian degeneration. *Nat Neurosci* 2009;12:387–389.
- 54 Valakh V, Frey E, Babetto E, Walker LJ et al. Cytoskeletal disruption activates the DLK/JNK pathway, which promotes axonal regeneration and mimics a preconditioning injury. *Neurobiol Dis* 2015;77:13–25.
- 55 Aquino JB, Musolino PL, Coronel MF et al. Nerve degeneration is prevented by a single intraneural apotransferrin injection into colchicine-injured sciatic nerves in the rat. *Brain Res* 2006;1117:80–91.
- 56 Hannus M BM, Engelmann JC, Weickert MT et al. siPools: Highly complex but accurately defined siRNA pools eliminate off-target effects. *Nucleic Acids Res* 1984;42:8049–8061.
- 57 Zhang K, Zhang L, Weinreb RN. Ophthalmic drug discovery: Novel targets and mechanisms for retinal diseases and glaucoma. *Nat Rev Drug Discov* 2012;11:541–559.
- 58 Meyer JS, Shearer RL, Capowski EE et al. Modeling early retinal development with human embryonic and induced pluripotent stem cells. *Proc Natl Acad Sci USA* 2009;106:16698–16703.
- 59 Osakada F, Ikeda H, Mandai M et al. Toward the generation of rod and cone photoreceptors from mouse, monkey and human embryonic stem cells. *Nat Biotechnol* 2008;26:215–224.
- 60 Williams RW, Strom RC, Rice DS et al. Genetic and environmental control of variation in retinal ganglion cell number in mice. *J Neurosci* 1996;16:7193–7205.
- 61 Patani R, Compton A, Puddifoot CA et al. Activin/Nodal inhibition alone accelerates highly efficient neural conversion from human embryonic stem cells and imposes a caudal positional identity. *PLoS One* 2009;4:e7327.
- 62 Nomura M, Li E. Smad2 role in mesoderm formation, left-right patterning and craniofacial development. *Nature* 1998;393:786–790.
- 63 Take-uchi M, Clarke JD, Wilson SW. Hedgehog signalling maintains the optic stalk-retinal interface through the regulation of Vax gene activity. *Development* 2003;130:955–968.
- 64 Masai I, Stemple DL, Okamoto H et al. Midline signals regulate retinal neurogenesis in zebrafish. *Neuron* 2000;27:251–263.
- 65 Wang SW, Kim BS, Ding K et al. Requirement for math5 in the development of retinal ganglion cells. *Genes Dev* 2001;15:24–29.
- 66 Brown NL, Patel S, Brzezinski J et al. Math5 is required for retinal ganglion cell and optic nerve formation. *Development* 2001;128:2497–2508.
- 67 Lupo G, Novorol C, Smith JR et al. Multiple roles of Activin/Nodal, bone morphogenetic protein, fibroblast growth factor and Wnt/beta-catenin signalling in the anterior neural patterning of adherent human embryonic stem cell cultures. *Open Biol* 2013;3:120167.
- 68 Bertacchi M, Lupo G, Pandolfini L et al. Activin/Nodal Signaling supports retinal progenitor specification in a narrow time window during pluripotent stem cell neuralization. *Stem Cell Reports* 2015;5:532–545.
- 69 Westenskow P, Sedillo Z, Barnett A et al. Efficient derivation of retinal pigment epithelium cells from stem cells. *J Vis Exp* 2015(97).
- 70 Sanvitale CE, Kerr G, Chaikwad A et al. A new class of small molecule inhibitor of BMP signaling. *PLoS One* 2013;8:e62721.
- 71 Bayramov AV, Eroshkin FM, Martynova NY et al. Novel functions of Noggin proteins: Inhibition of Activin/Nodal and Wnt signaling. *Development* 2011;138:5345–5356.
- 72 Kuwahara A, Ozone C, Nakano T et al. Generation of a ciliary margin-like stem cell niche from self-organizing human retinal tissue. *Nat Commun* 2015;6:6286.

73 Du Y, Xiao Q, Yip HK. Regulation of retinal progenitor cell differentiation by bone morphogenetic protein 4 is mediated by the smad/id cascade. *Invest Ophthalmol Vis Sci* 2010;51:3764–3773.

74 Venugopalan P, Wang Y, Nguyen T et al. Transplanted neurons integrate into adult retinas and respond to light. *Nat Commun* 2016;7:10472.

75 Chamling X, Sluch VM, Zack DJ. The potential of human stem cells for the study and treatment of glaucoma. *Invest Ophthalmol Vis Sci* 2016;57:ORSF1-6.

76 Badea TC, Williams J, Smallwood P et al. Combinatorial expression of Brn3 transcription factors in somatosensory neurons: Genetic and morphologic analysis. *J Neurosci* 2012;32:995–1007.

77 Badea TC, Cahill H, Ecker J et al. Distinct roles of transcription factors brn3a and brn3b in controlling the development, morphology, and function of retinal ganglion cells. *Neuron* 2009;61:852–864.

78 Schmidt TM, Chen SK, Hattar S. Intrinsically photosensitive retinal ganglion cells: Many subtypes, diverse functions. *Trends Neurosci* 2011;34:572–580.



See www.StemCellsTM.com for supporting information available online.